

1 **Kinetic study of colored species formation during paracetamol removal from**
2 **water in a semicontinuous ozonation contactor**

3

4 N. Villota¹, J.I. Lombraña², A. Cruz-Alcalde^{3*}, M. Marcé³, S. Esplugas³

5

6 ¹ Department of Chemical and Environmental Engineering, Escuela Universitaria de
7 Ingeniería de Vitoria-Gasteiz, University of the Basque Country UPV/EHU, Nieves
8 Cano 12, 01006 Araba, Spain

9

10 ² Department of Chemical Engineering, Faculty of Science and Technology, University
11 of the Basque Country UPV/EHU, Barrio Sarriena s/n, 48940 Bizkaia, Spain

12

13 ³ Department of Chemical Engineering and Analytical Chemistry, Faculty of Chemistry,
14 Universitat de Barcelona, C/Martí i Franqués 1, 08028 Barcelona, Spain

15

16 *Corresponding author: alberto.cruz@ub.edu, Tel: +34934029789; fax: +34934021291

17

18 **ABSTRACT**

19

20 Paracetamol aqueous solutions, when ozonized, acquired a strong red coloration
21 depending on the applied ozone dose and the initial pH of the aqueous solution. Then,
22 this color loses intensity and turns to yellow. Color formation is favored when operating
23 at initial pH₀=12.0 and ozone flow-rate 4.2 mg/min. A mechanism describing color
24 formation was proposed, being the main pathway involved an initial paracetamol
25 hydroxylation to yield 3-hydroxyacetaminophen followed by the formation of 2-amino-

26 5-hydroxyacetofenone. Then, these compounds are degraded to colored oxidation by-
27 products. A model describing color evolution was also proposed, considering first-order
28 kinetics for both color formation and degradation. The corresponding kinetic constant
29 values were determined to be $k_f=0.01$ (1/min) and $k_d=0.03 \text{ pH}-0.055$ (1/min),
30 respectively. A relationship between aromaticity loss and color changes during the
31 reaction has been estimated considering the parameter $\alpha=k_A/k_f$, being $\alpha=1.62 \text{ pH} + 3.5$
32 and the first-order rate constant for aromaticity loss given by $k_A=0.0162 \text{ pH} + 0.035$
33 (1/min).

34

35 **KEYWORDS**

36

37 Chemical pathway; Color; Kinetic modelling; Ozone; Paracetamol; Initial pH

38

39 **1. Introduction**

40

41 Among the so called contaminants of emerging concern, pharmaceuticals stand out as
42 one of the most detected families of compounds in wastewater effluents, but also in
43 surface waters and drinking waters (Mompelat et al., 2009; Richardson, 2009; Seifrtová
44 et al., 2009; Sun et al., 2014). These pollutants enter the water resources by means of
45 industrial, agricultural and domestic residual effluents that are transported to wastewater
46 treatment plants (WWTPs), where many of them –because of their chemical properties–
47 cannot be effectively eliminated by the conventional treatment technologies typically
48 implemented in those facilities (Blair et al., 2015; Baalbaki et al., 2016). Current
49 research focus on the development of chemical processes able to degrade recalcitrant

50 chemicals from wastewater effluents and natural water compartments, in order to avoid
51 their presence in urban water distribution networks (Ziylan-Yavaş and Hince, 2018). In
52 this context, Advanced Oxidation Processes (AOPs) are considered a promising
53 alternative (Hollender et al., 2009; Rosario-Ortiz et al., 2010; Oller et al., 2011; Margot
54 et al., 2013; Lee et al., 2016).

55

56 This work focused on the study of paracetamol (4-hydroxyacetanilide, 4-
57 acetamidephenol or acetaminophen) degradation by means of ozonation. This
58 pharmaceutical is employed as anti-inflammatory and analgesic (Skoumal et al., 2006)
59 and, despite human organism is capable of metabolizing up to a 90% of the consumed
60 drug –excreting only a 3-5%– (Ellenhorn and Barceloux, 1988; McEvoy, 1992), the
61 worldwide amount of this chemical reaching WWTPs have been estimated to be in the
62 range of 292-585 ton/year (El Najjar et al., 2014). Moreover, this pollutant has been
63 often found in municipal sewage effluents at concentrations up to 65 µg/L (Villaroel et
64 al., 2014). Although the concentration of paracetamol detected in natural waters is
65 generally below the µg/L range (Skoumal et al., 2006), its presence may potentially
66 affect aquatic organisms (Santos et al., 2010) due to the ability of this chemical to
67 bioaccumulate (Radjenović et al., 2009; Deblonde and Hartemann, 2013; Valdés et al.,
68 2014; Zenker et al., 2014). Studies reported in the bibliography show that AOPs are
69 usually effective treatments for degrading this kind of organic pollutants from water
70 (Ay and Kargi, 2001). In addition, and due to the low concentrations of these substances
71 in water matrices, membrane technology can be used to concentrate micropollutants
72 prior to AOPs treatments reducing the volume of water to treat (Savchuk and Krizova,
73 2015).

74

75 Ozone is a powerful oxidant employed in drinking and wastewater treatment plants due
76 to its ability for microorganisms inactivation and both inorganic and organic
77 contaminants transformation (Paraskeva and Graham, 2002; Rodríguez et al., 2008;
78 Gomes et al., 2017). However, the application of ozone presents some practical
79 limitations related to operational pH: under acidic conditions, O₃ is relatively stable and
80 directly reacts with pollutants, whereas for pH values corresponding to neutral and basic
81 conditions this oxidizing species decomposes to highly oxidizing radicals (*i.e.*, hydroxyl
82 radicals •OH) that enhance the process efficiency (Rodríguez et al., 2017). In addition,
83 the physicochemical properties (*i.e.*, pK_a and second-order rate constants with O₃ and
84 OH•) of micropollutants determine their removal efficiencies according to the medium
85 pH, which can be different depending on the wastewater origin. Therefore, it is
86 interesting to perform a study that covers a wide range of operational pH. Furthermore,
87 it is necessary to ensure a reduction in the toxicity of the ozonized effluents, which is
88 normally attributed to the toxic character of the transformation products generated
89 because of the treatment application (Wert et al., 2007; Lee and von Gunten, 2016;
90 Maya et al., 2018). Thus, in order to ensure the treatment effectiveness, it is necessary to
91 perform a complete study of the process assessing reaction kinetics, transformation
92 products and toxicity of the treated water (Cruz-Alcalde et al., 2017).

93

94 During organic matter ozonation, a reduction in the relative amount of aromatic rings
95 and conjugated bonds contained in the water matrix is produced. Also, the number of
96 electron acceptors (*i.e.*, carboxyl, carbonyl, hydroxyl, alcoxy) increases (Swietlik and
97 Sikorska, 2004). Ozone preferently degrades organic molecules with low oxidation state
98 (low O/C ratio) and a high degree of insaturation (high H/C ratio), yielding more
99 saturated and oxygenated (alcohols, aldehydes, carbonyls, ketones and carboxylic acids)

100 (Reemtsma and These, 2005; von Gunten, 2003). Among them, the relative amount of
101 carboxylic acids generated during the process is generally much higher than that of
102 aldehydes or ketones (Nawrocki and Kasprzyk-Hordern, 2003). They typically are
103 compounds with short molecular chains (less than 5 C atoms), such as formic, acetic or
104 oxalic acid (Can and Gurol, 2003).

105

106 During paracetamol ozonation, aqueous solutions of this chemical acquire a red tonality
107 which gradually turns to yellow. In the present work, therefore, and since color is an
108 important organoleptic parameter determining water quality (Villota et al., 2016),
109 degradation intermediates causing this change of tone in water have been identified.
110 According to the transformation products detected through LC-MS, the oxidation
111 mechanism taking place simultaneously to the mentioned color changes in paracetamol
112 solutions has been proposed. Moreover, the influence of main operational parameters of
113 ozonation process (*i.e.*, initial pH and applied ozone flow-rate) on color formation,
114 degree of mineralization and aromaticity, as well as on the mass transfer of ozone to the
115 aqueous phase, has been studied including some toxicity studies (El Najjar et al., 2014).
116 By this way, operational conditions leading to the formation of chromophoric
117 intermediate (quinone compounds) increasing water toxicity have been characterized
118 (Mijangos et al., 2006).

119

120 **2. Materials and methods**

121

122 **2.1. Chemicals and reagents**

123

124 Paracetamol solutions $[Pa]_0=50.0$ mg/L were prepared by dissolving pure paracetamol
125 (Sigma-Aldrich 99.9%) in milli-Q water produced by a filtration system (Millipore,
126 USA). Assays were performed operating under different initial pH conditions (pH_0
127 between 3.0 and 12.0) in order to assess the effect of this parameter on color formation
128 during ozonation of paracetamol aqueous solutions. This range was selected to cover a
129 wide range of water properties. The initial pH was adjusted by adding a few drops of
130 concentrated HCl and NaOH solutions in order to avoid sample dilution. Although the
131 operational pH has not been controlled during the reaction, its maximum variation has
132 been less than 0.5 pH units (Mijangos et al., 2006). Pure oxygen ($\geq 99.999\%$) for ozone
133 production was supplied by Abelló Linde (Spain). The reproducibility of the ozonation
134 assays was considered based on the mean of the colour of the values measured,
135 obtaining standard deviations less than 5% in all cases.

136

137 **2.2. Semicontinuous ozonation setup**

138

139 For each ozonation experiment, 1.0 L of paracetamol solution was prepared and added
140 into a jacketed reactor operating in semi-continuous mode. Experiments were performed
141 at a constant temperature of 25.0 °C, maintained by means of a thermostatic bath.
142 Ozone/oxygen gaseous mixtures were generated by means of a 301.19 Labor Ozonator
143 (Sander, Germany) and injected at the bottom of the reactor employing a metallic
144 difusser (pore size: 10 μ m). The ozone flow rate applied was in the range 4.2 - 25.0
145 mg/min. The medium was under stirring conditions in order to ensure homogeneity. The
146 inlet and outlet ozone concentration in the gas phase were measured by means of two
147 BMT 964 ozone analyzers (BMT Messtechnik GMBH, Germany), placed up and
148 downstream the contactor, respectively. More information about the experimental setup

149 may be found elsewhere (Marcé et al., 2016). The dissolved ozone concentration was
150 measured by the Indigo colorimetric method (Bader and Hoigné, 1981; Greenberg et al.,
151 1999).

152

153 **2.4. Analytical procedures**

154

155 Paracetamol mineralization was estimated through total organic carbon (TOC, mgC/L)
156 measurements using a TOC-VCSN Shimadzu Analyzer. Color was determined using an
157 UV/Vis spectrophotometer (DR 6000-Hach Lange) by direct measurement of the
158 samples absorbance at $\lambda=455$ nm (Mijangos et al., 2006). For aromaticity loss
159 monitoring, UV absorbance measurements were performed at $\lambda=254$ nm. The samples
160 were analyzed by Liquid Chromatography-Mass Spectrometry (LC-MS) to elucidate the
161 paracetamol degradation pathways that induce high levels of color in the water during
162 the ozonation process. Samples were analyzed by HPLC coupled in series to a MS-TOF
163 (G3250AA by Agilent, USA) system and a UV detector (1100 Agilent). This
164 configuration allowed the comparison between chromatograms obtained through UV
165 and MS detectors, discarding this way interferences caused by artifacts.

166 MS data were collected in full scan mode (50–1500 m/z), employing negative
167 electrospray ionization. The column employed was a Teknokroma Mediterranea Sea 18
168 (250 mm \times 4.6 mm and 5 μ m size packing). The mobile phase consisted of a 65:35
169 volumetric mixture of methanol and Milli-Q water acidified at pH 3.0 by the addition of
170 H₃PO₄. The flow rate was maintained at 0.3 mL min⁻¹ and the detection wavelength (for
171 the UV detector) was set to 200 nm and 243 nm. The spectrophotometer conditions
172 were voltage of capillary 3500 V and shredder 125 V, being the limit of detection
173 (LOD) 0.25 μ M.

174

175 **3. Results and discussion**

176

177 **3.1. Effect of applied ozone flow-rate on color formation**

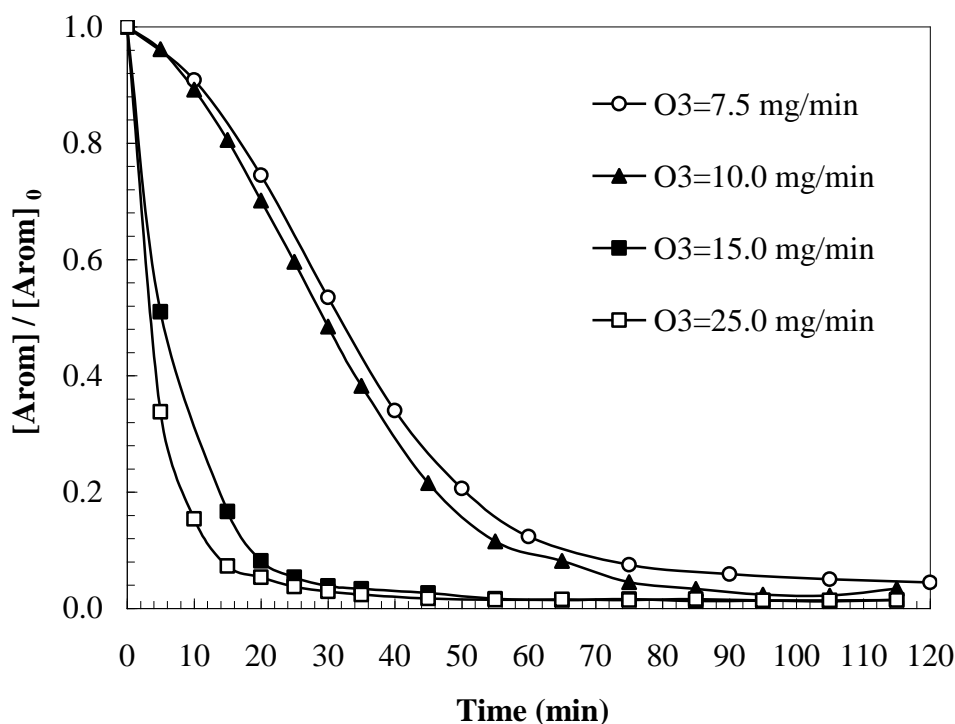
178

179 During the ozonation of aqueous solutions of paracetamol, a general aromaticity loss in
180 the reaction medium is observed (Fig. 1). This fact confirms organic matter oxidation,
181 leading to changes in molecular structures of species initially contained in the water
182 matrix. During ozonation treatment, the highest absorption observed in the UV
183 spectrum corresponds to the opening of aromatic rings causing the transformation of
184 organic molecules (Xiong and Legube, 1991). This reaction is fast and it is
185 characterized by the decrease of UV absorbance measured at 254 nm (von Gunten,
186 2003).

187

188 Results show a total loss of the aromaticity in the water produced when ozonation of
189 50.0 mg/L paracetamol solutions employing ozone flow rates higher than 7.5 mg
190 O₃/min is applied. It is also observed that an increase of ozone flow-rate causes an
191 increase in the rate of aromaticity reduction. However, this increase does not follow a
192 linear tendency, which would indicate the existence of particular operation conditions
193 leading to the activation of different degradation pathways through which the overall
194 oxidation mechanism of paracetamol takes place.

195



196

197 **Fig. 1.** Influence of the inlet ozone flow rate during paracetamol oxidation experiments
 198 on aromaticity loss. Experimental conditions: $[Pa]_0=50.0$ mg/L; $pH_0=12.0$; $T=25.0^\circ\text{C}$.

199

200 Simultaneously to aromaticity loss, color changes in oxidized waters also take place,
 201 indicating the kinetic evolution of a reaction intermediate (Fig. 2). Initially, colorless
 202 aqueous solutions containing paracetamol Color_0 (AU) gradually acquire a strong red
 203 tonality, until the maximum color intensity $\text{Color}_{\text{max}}$ (AU) is reached at a certain
 204 reaction time t_{max} (min). Then, color acquires a yellowish tone with time-decreasing
 205 intensity until a residual value of this parameter is reached (Color_∞ , AU). This fact
 206 would indicate the simultaneous cleavage of paracetamol molecules and subsequent
 207 formation of chromophoric groups –such as $-\text{C}=\text{O}$, $-\text{C}=\text{C}$ y NO_2- – in the respective
 208 structures of the degradation products.

209

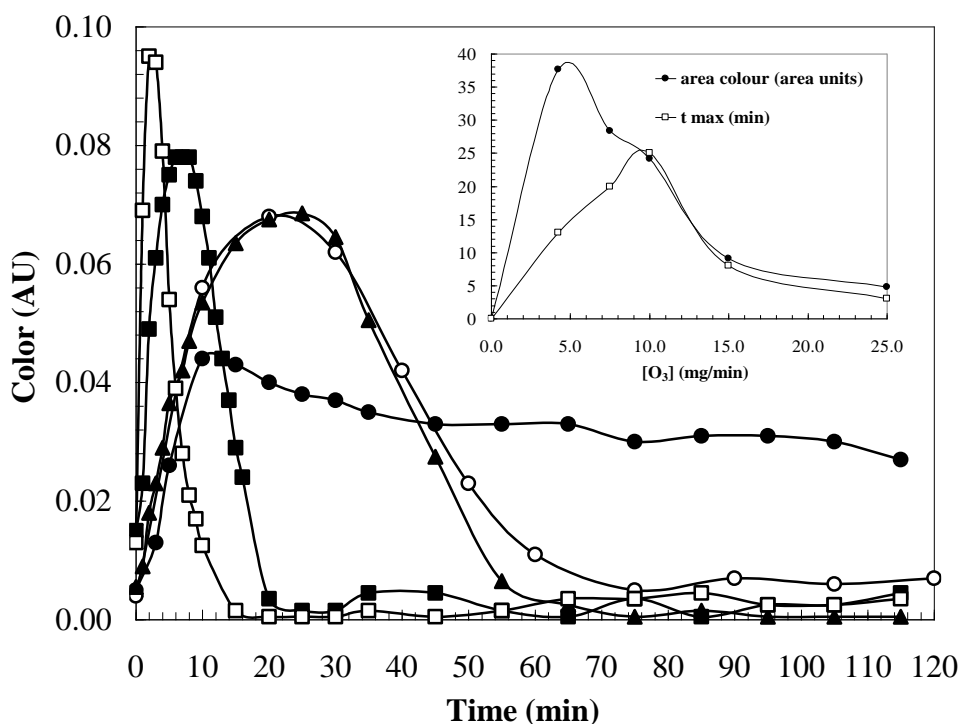
210 Observed changes in color show an asymmetric bell-shaped tendency, with the
 211 decreasing part of this curve presenting a tail. This evolution can be explained by the

212 two stages taking place during ozonation of paracetamol (El Najjar et al., 2014). The
213 first of these regimes, characterized by exhibiting fast oxidation kinetics, occurs during
214 the first minutes of the process. During this period, in which a loss in water aromaticity
215 is observed, paracetamol is oxidized to yield different reaction intermediates, some of
216 them containing chromophoric terminations responsible for color appearance in the
217 water matrix. Then, a slower ozonation stage starts to take place. At this point of the
218 process, reaction intermediates –including colored species are slowly degraded to
219 smaller molecules, ultimately leading to the formation of colorless carboxylic acids (i.e.,
220 oxalic, acetic and formic).

221

222 In order to analyze the effect of ozone flow-rate on color formation and degradation
223 kinetics, the color signal (in color area units) as a function of the ozone flow-rate inlet
224 has been represented (see Fig. 2). These results allow checking how, regardless of the
225 employed operational conditions, paracetamol ozonation always leads to intermediates
226 containing chromophoric groups in their molecular structures. However, colored species
227 formation is better observed under low inlet ozone flow-rates ($[O_3]=4.2$ mg/min). When
228 gradually increasing this dosing rate up to 25.0 mg/min, color curves with smaller areas
229 are registered due to faster formation and degradation of chromophoric reaction
230 intermediates.

231



232

233 **Fig. 2.** Effect of flow rate of ozone applied during paracetamol oxidation on the color
 234 appearance in water matrices. Experimental conditions: $[Pa]_0=50.0$ mg/L; $pH_0=12.0$;
 235 $T=25.0^\circ C$. Legend: Inlet flow rate of ozone $[O_3]=$ ● 4.2 mg/min, ○ 7.5 mg/min, ▲ 10.0
 236 mg/min, ■ 15.0 mg/min, □ 25.0 mg/min.

237

238 To explain this phenomenon, it is necessary to analyze the reaction time –as a function
 239 of the volumetric ozone flow-rate– for which the maximum color intensity in water
 240 matrix is observed (t_{max} , min). This is shown in Fig. 2. This t_{max} parameter does not
 241 proportionally decrease with increasing ozone flow-rate. Instead, a maximum is
 242 observed for certain operational conditions, which would indicate that ozone does not
 243 exert a catalytic effect in oxidation but determines the degradation yield of paracetamol
 244 leading to colored species formation.

245

246 The ozone flow-rate employed during the process produces a selective paracetamol
 247 oxidation to yield colored species through different degradation routes. The overall
 248 degradation mechanism does not consist of a unique degradation via leading to the

249 generation of a single compound. On the contrary, a mix of chemical species coexists in
250 the system. Therefore, the observed color kinetics would be caused by reaction
251 intermediates presenting different molecular structures. The time for which the
252 maximum color intensity is registered would indicate the generation of a group of
253 predominant colored species, as well as the oxidative level in which these compounds
254 are formed throughout the overall degradation mechanism.

255

256 **3.2. Pathway of colored intermediates generation**

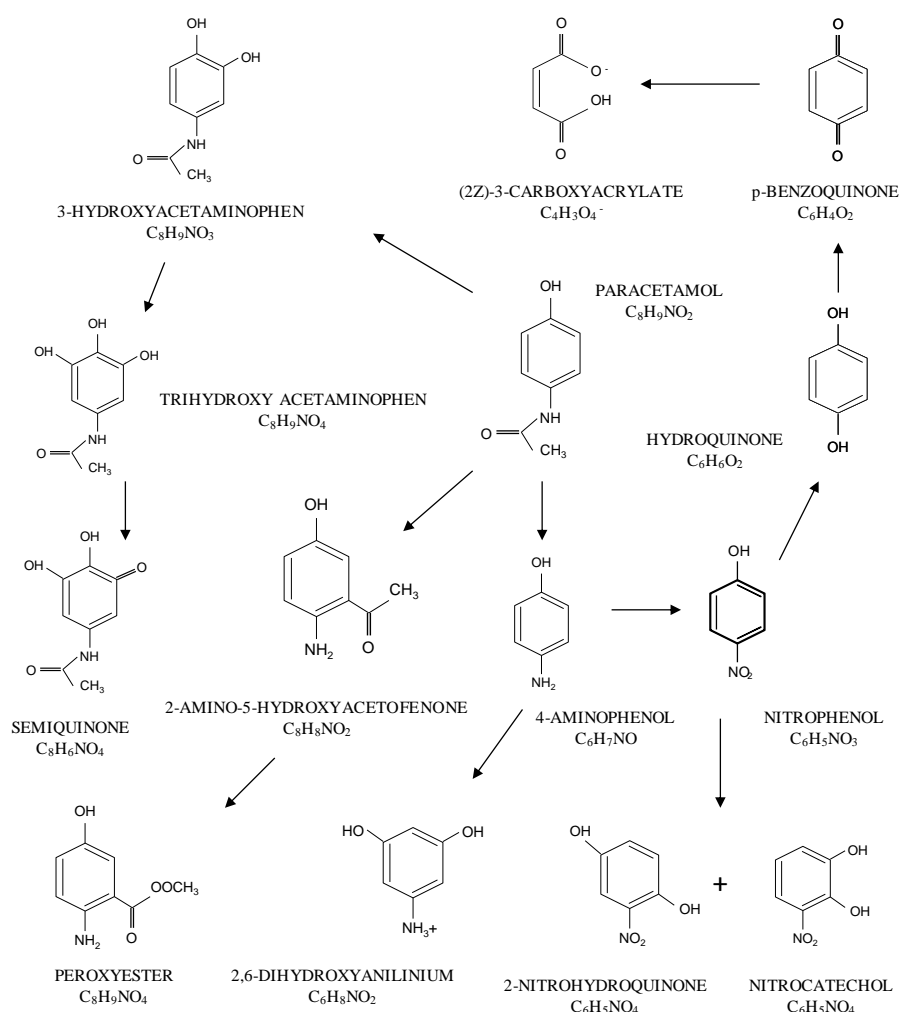
257

258 Ozonized aqueous solutions of paracetamol ($[Pa]_0=50.0$ mg/L) corresponding to
259 experiments with an ozone flow-rate of 4.2 mg/min and $pH_0=12.0$ as experimental
260 conditions, have been analyzed by LC-MS to determine the nature of intermediates
261 causing color in water. These are the operational conditions for which a higher color
262 intensity remained in the residual water ozonized that makes possible to analyze the
263 compounds contained in the colored water. In this situation, therefore, the formed
264 chromophoric intermediates could be analyzed before their subsequent transformation
265 to colorless acids. On the basis of the obtained results, and considering the degradation
266 mechanisms of paracetamol reported in scientific literature, (He et al., 2018; Villota et
267 al., 2018; Villota et al., 2016; Martignac et al., 2013; Moctezuma et al., 2012), an
268 scheme of those reactions causing color generation in ozonized waters has been
269 proposed (Fig. 3).

270

271 The nature of the detected ozonation by-products depends on the employed flow-rate of
272 ozone. Previous works show that employing lower ozone dosages and high substrate
273 concentrations leads to the detection of reaction intermediates containing from 4 to 6 C

274 atoms, whereas employing elevated ozone dosages favored the formation of smaller
 275 molecules generally containing 1-3 C atoms (Brunet et al., 1982). For the current case
 276 of study, therefore, the color observed during paracetamol ozonation operating at flow-
 277 rates lower than the stoichiometric value, may be induced by intermediate species
 278 exhibiting molecular structures with 4-6 carbon atoms.
 279



280

281

282 **Fig. 3.** Reaction intermediates generated during the ozonation of paracetamol aqueous
 283 solutions. Experimental conditions: [Pa]₀=50.0 mg/L; pH₀=12.0; [O₃]=4.2 mg/min;
 284 T=25.0°C.

285

286 Analysis on the colored reaction mixture would indicate the formation of some
287 transformation products such as hydroquinone, benzoquinone, p-aminophenol and p-
288 nitrophenol. In accordance with the suggested mechanism, three reactions involving the
289 initial attack of formed hydroxyl radicals (HO•) to finally yield ortho-meta- and para-
290 hydroxylated compounds (with respect to the initial hydroxyl group of paracetamol)
291 would compete to simultaneously take place in the system. Existent works dealing with
292 this subject have reported that, during the initial stages of the oxidation process,
293 hydroxyl and amino groups present a high reactivity towards ortho- and para- positions,
294 due to the high electron-donating capacity exhibited by these moieties (Westerhoff et
295 al., 1999). Contrarily, reactions occurring at meta- positions are less favored and,
296 therefore, hydroxylation reactions at this point of the aromatic ring are considered to be
297 of minor relevance (Vogna et al., 2002).

298

299 Oxidation could be initiated via hydroxyl radical addition to the ortho-position of
300 paracetamol, leading to the formation of 3-hydroxyacetaminophen. The predominant
301 pathway, however, is the one initiated by the generation of the paracetamol isomer 2-
302 amino-5-hydroxyacetophenone. This reaction implies the migration of an acetyl group
303 from the amino moiety of paracetamol in position para- (with respect to the hydroxyl
304 group) to position ortho- (in the aromatic ring) with respect to the amino (-NH₂) group.

305

306 The presence of p-aminophenol and p-nitrophenol in the colored mixture has been also
307 detected. This fact would indicate a deacylation mechanism, subsequently leading to the
308 generation of an amide group bonded to the aromatic ring (Bahnemann et al., 2007).
309 Due to the fact that hydroxyl radicals mainly react through addition to the aromatic ring,
310 p-nitrophenol would be generated by oxidation of p-aminophenol. First, the addition of

311 HO[•] to the aromatic ring would be produced, followed by the elimination of a hydroxyl
312 group. Then, a deprotonation of the formed radical cation would generate an easily
313 oxidizable aniliny radical, to finally yield p-nitrophenol (Martignac et al., 2013).

314

315 During p-nitrophenol oxidation, two competitive chemical transformations could take
316 place: an hydroxylation in ortho- position to finally yield nitrocatechol, on one hand,
317 and a hydroxylation in para- position (with respect to the phenolic hydroxyl group) and
318 later elimination of the nitro group, obtaining by means of this way hydroquinone as
319 product (Moctezuma et al., 2007). Further hydroquinone oxidation would finally yield
320 benzoquinone.

321

322 **3.3. Influence of initial pH and oxidant dosage on ozonized water coloration**

323

324 Color formation in ozonized water has been analyzed, considering both the pH₀ (Fig. 4)
325 and ozone flow-rate ([O₃] mg/min), (Fig. 5) employed during ozonation assays. The aim
326 of this study was to determine whether the degradation route causing color formation
327 consisted of a direct ozone oxidation of paracetamol or, on the contrary, could be
328 attributed to the unselective oxidation by hydroxyl radicals generated through ozone
329 decomposition (pH₀ values higher than 6.0). This part of the work was performed
330 operating within an initial pH range of 3.0-12.0 (see Fig. 4). Normalized TOC (mg/L)
331 and absorbance at 254 nm ([Arom], AU) values, together with the color (Color_∞, AU)
332 and the ozone mass transfer coefficient (K_{La}, l/min) determined at the end of treatment
333 have been all represented. The maximum color generated during ozonation experiments
334 has been also included.

335

336 The determination of ozone transfer parameters may be done according to the equations
 337 of gas-liquid mass transfer (Rodriguez et al., 2017). Ozone consumption N_{O_3} (mg/L
 338 min) can be expressed as the volumetric mass transfer coefficient K_{La} (1/min)
 339 multiplied by the mass transfer driving force, according to Eq. 1. The volumetric mass
 340 transfer coefficient has been estimated considering the mass transfer taking place from
 341 gas to liquid phase, being C_i (mol/L) the ozone concentration at the interphase, C_L
 342 (mg/L) in the liquid phase and C_L^* in the liquid phase in equilibrium with the gas
 343 (mg/L). Note that in Eq. 1 K_{La} (1/min) is the global mass transfer coefficient, whereas
 344 k_{Ga} and k_{La} represent the individual coefficients for gas and liquid phases, respectively.

345

$$346 \quad N_{O_3} = K_{La} (C_L^* - C_L) = k_{Ga} H (C_L^* - C_i) = k_{La} (C_i - C_L) \quad (1)$$

347

348 Ozone mass transfer can be also expressed as a function of the ozone flow rate (Q_{O_3} ,
 349 L/min), the reaction volume (V , L) and the difference between the inlet and outlet ozone
 350 concentrations in the gas phase ($C_{G,in}$ and $C_{G,out}$ (mg/L), respectively) (see Eq. 2). It is
 351 worth to mention here that transferred ozone can be accumulated in the liquid phase or
 352 be consumed through two main mechanisms: direct oxidation reactions with the
 353 contaminant (R_{O_3} , mg/L min), or O_3 self-decomposition leading to the generation of
 354 hydroxyl radicals (r_{O_3} , mg/L min).

355

$$356 \quad N_{O_3} = \frac{Q_{O_3}}{V} (C_{G,in} - C_{G,out}) = K_{La} (C_L^* - C_L) = \frac{dC_L}{dt} + R_{O_3} + r_{O_3} \quad (2)$$

357

358 Ozone concentration in the liquid phase in equilibrium with gas phase can be estimated
359 considering the Henry Law (Eq. 3), where H (atm/ozone molar fraction in the liquid) is
360 the Henry constant and P_G (atm) is the partial pressure of ozone in the gas phase.

361

$$362 \quad C_L^* = \frac{P_G}{H} \quad (3)$$

363

364 The Henry constant has been determined as a function of the liquid phase temperature
365 (K) and pH, according to Eq. 4 (Roth and Sullivan, 1981).

366

$$367 \quad H = 38 \cdot 10^6 C_{OH^-}^{0.035} \exp\left(\frac{-2428}{T}\right) \quad (4)$$

368

369 Obtained results allow checking how both aromaticity loss and residual color of
370 ozonized waters do not experiment important variations with the medium pH_0 .
371 However, the maximum color generated in water shows a strong dependence from pH:
372 when operating in the initial pH range comprised between 3.0 and 6.0, this intensity
373 remains constant, whereas if this parameter is increased from 6.0 to 12.0, a potential rise
374 in its value is observed. To explain these results, it is necessary to consider the
375 Henderson-Hasselbach equation concerning the ionization curve of paracetamol. When
376 water pH is increased, the concentration of hydroxide anions in the system also
377 increases, and consequently does the ozone decomposition to hydroxyl radicals. This
378 fact causes an enhancement in the oxidizing capacity of the system, leading to a higher
379 degradation efficiency of the pharmaceutical to yield colored transformation products.

380

381 On the other hand, paracetamol is a weak acid, with a pKa value equal to 9.38
382 (Dastmalchi et al., 1995). This is going to determine the reactivity of this compound.
383 When assays are performed within the operational pH interval comprised between 3.0
384 and 9.4, as the system is acidified, the number of non-dissociated or non-ionized
385 molecules is relatively larger. On the contrary, for pH values higher than 9.4 (under
386 basic conditions) the proportion of dissociated molecules increases. This fact could
387 explain the strong color rise observed when operating at a pH value of 12.0, since
388 paracetamol molecules under these conditions exhibit a high degree of dissociation.
389 Because of this, this specie is degraded through oxidative routes conducting to the
390 generation of chromophoric structures that provide color to the ozonized water.

391

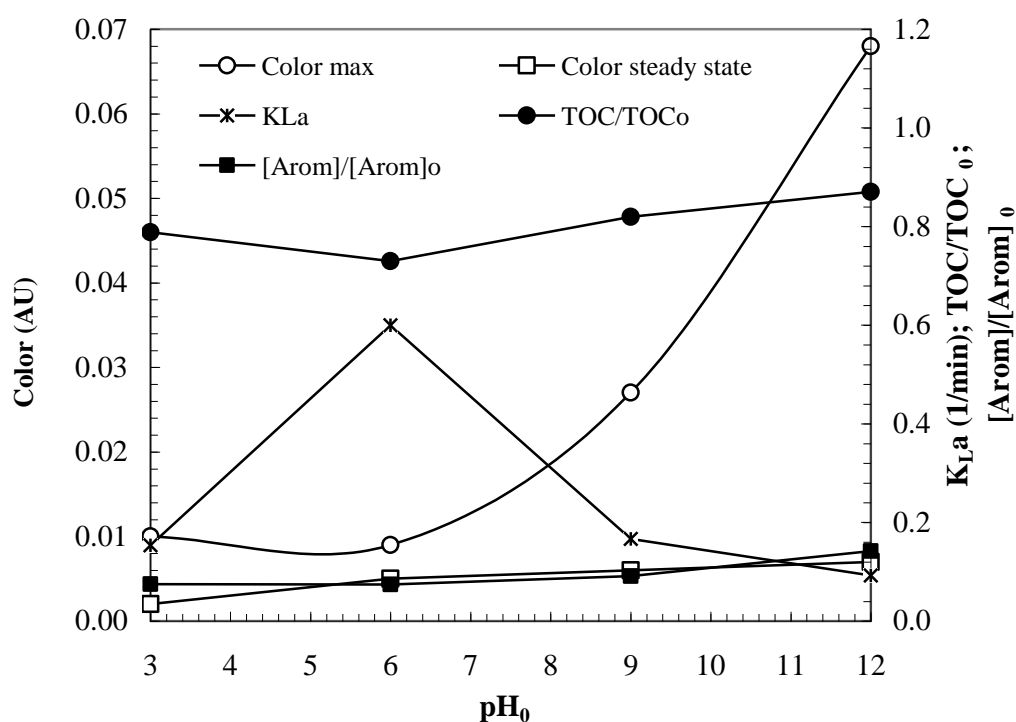
392 As indicated in the relationship by Roth and Sullivan, 1981, if the system pH is
393 increases this favors the ozone transfer to the reacting solution. However, obtained
394 results in the current case of study suggest that the ozone transference to aqueous
395 solutions of paracetamol is maximum when the process is performed at a pH value of
396 6.0. This phenomenon is accompanied by a decrease in the total organic carbon (TOC,
397 mg/L). To explain this phenomenon, it is necessary to consider the nature of chemical
398 species that are present in the reaction medium, since they can either accelerate the
399 decomposition of ozone to hydroxyl radicals (radical chain reactions) or slowing it
400 down. In this case, the pKa value for paracetamol (9.4) determines the process
401 performance. The more acidic is the media the higher is the number of non-dissociated
402 paracetamol molecules. On the contrary, at $\text{pH} > \text{pKa}$ conditions, the number of
403 unprotonated molecules becomes larger. This fact can considerably impact the ozone
404 reactivity with this pharmaceutical. In addition, when operating within a pH range

405 between 6.0 and 12.0, the ozone concentration in water increasingly diminishes due a
406 higher concentration of hydroxide (OH^-) ions.

407

408 This clearly affects the ozone transfer to the liquid phase, which is reflected in lower
409 K_{La} values with increasing pH values. In addition to the effect exerted by the hydroxide
410 ion, it is possible that, because of paracetamol mineralization, some inorganic species
411 (mainly nitrogen anions) could be formed. These ions would act as ozone and radical
412 scavengers, also affecting the ozone transfer to the liquid phase (Gottschalk et al., 2010;
413 Sumegova et al., 2013).

414



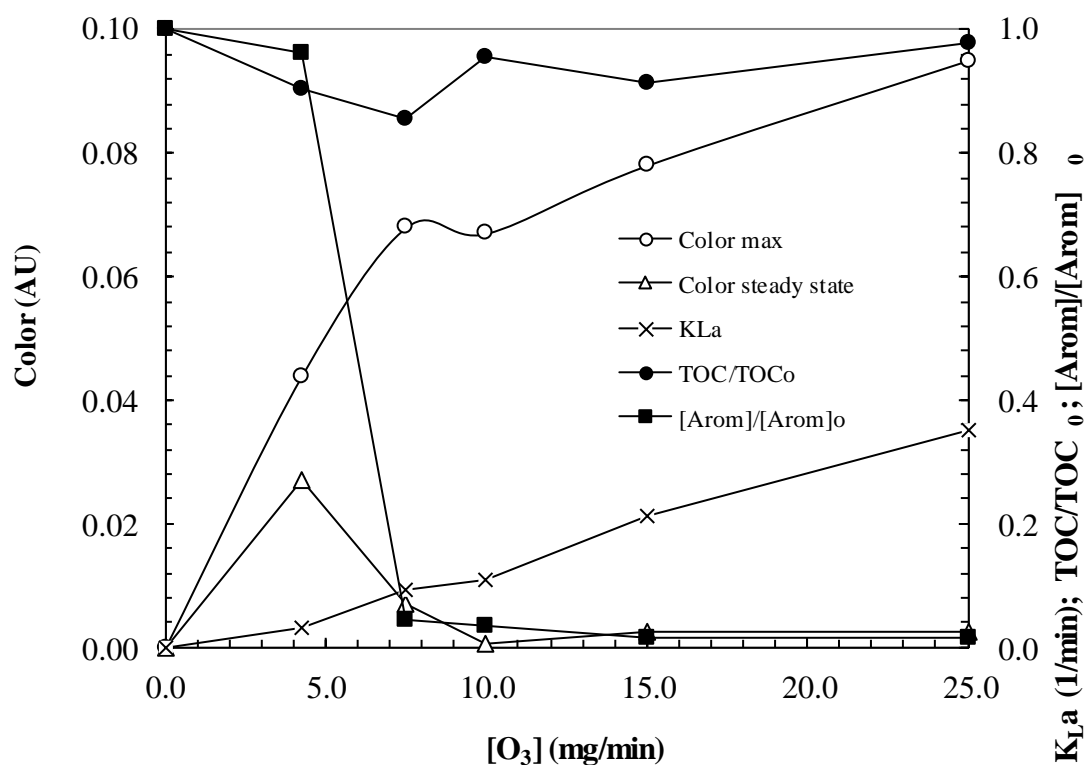
415

416 **Fig. 4.** Influence of initial pH on color (AU) formation, mass transfer coefficient K_{La}
417 (1/min), organic matter mineralization TOC/TOC_0 and aromaticity loss
418 ($[\text{Arom}]/[\text{Arom}]_0$) during paracetamol ozonation. Experimental conditions: $[\text{Pa}]_0=50.0$
419 mg/L ; $[\text{O}_3]=4.2 \text{ mg/min}$; $T=25.0^\circ\text{C}$; $t=120 \text{ min}$.

420

421 The influence of the employed ozone dose was evaluated in ozonation assays carried
422 out at pH=12.0. As mentioned, these conditions potentiate the formation of colored
423 structures (Fig. 5). In this case, aromaticity loss exhibits a strong dependence with
424 ozone dose: when working at ozone flow rate below 4.2 mg/min for a total reaction time
425 of 2 h, the aromaticity reduction is less than 4%. If on the contrary, the oxidant flow rate
426 is increased up to 7.5 mg/min, an abrupt drop of this parameter (approximately a 95%)
427 is observed. The oxidant/substrate ratio corresponding to these experimental conditions,
428 $57 \text{ mol O}_3/\text{mol C}_8\text{H}_9\text{NO}_2$, would therefore correspond to that stoichiometric relationship
429 required in order to produce a reduction in the aromaticity of the paracetamol
430 molecules. If ozone flow-rate is further increased, the observed final percentage of
431 aromatic species in solution is less than 5%. From this point, the depletion of this
432 residue follows a linear behavior with the ozone dose increment: for an ozone flow rate
433 of 1.0 L/min, for instance, water aromaticity reduction is 99%.

434



435
436

437 **Fig. 5.** Effect of ozone flow rate during paracetamol oxidation on color formation (AU),
438 mass transfer coefficient K_{La} (1/min), organic matter mineralization TOC/TOC₀ and
439 aromaticity loss ($[Arom]/[Arom]_0$). Experimental conditions: $[Pa]_0=50.0$ mg/L;
440 $pH_0=12.0$; $T=25.0^\circ C$; $t=120$ min.

441

442 Ozone transference to the aqueous solution increases with increasing inlet ozone flow-
443 rates, but only if operation pH is constant. This enhancement in the gas-liquid transfer
444 leads to an increase of the water-color formation. This phenomenon appears to indicate
445 that pH conditions define the selectivity ozonation mechanism, while the efficiency of
446 paracetamol degradation leading to colored species formation would be more influenced
447 by the applied ozone doses.

448

449 It has been verified that a residual coloration lasts in ozonized waters when the provided
450 ozone flow-rate is 4.2 mg/min. That color is less intense when the inlet flow of ozone is
451 7.5 mg/min. This maximum intensity value of the residual color would indicate that,

452 when operating at ozone doses below the stoichiometric relationship of 1/57 (mol
453 paracetamol/mol ozone), the amount of oxidant provided to the system would not be
454 enough to produce those significant alterations in the aromatic structures of paracetamol
455 subsequently leading to a noticeable reduction in water aromaticity. Because of this, an
456 aromatic chromophoric residue –conferring that characteristic color to the medium–
457 persists in the treated waters.

458

459 **3.4. Kinetic model for water coloration**

460

461 The kinetic model suggested in the present study relates the aromaticity loss of ozonized
462 paracetamol solutions with changes in color observed in the water matrix. In order to
463 model aromaticity loss, in first place, a mathematical model based on the scheme shown
464 in Fig. 1 has been considered. Thus, it is assumed that paracetamol ozonation process
465 leads to the generation of transformation products exhibiting less aromaticity than the
466 parent compound. The aromaticity reduction rate is given by the corresponding first-
467 order kinetic constant k_A (1/min).

468



470 With,

471

472 k_A : first-order kinetic constant describing aromaticity loss in aqueous solutions
473 of paracetamol during ozonation process (1/min)

474

475 In accordance with Eq. 5, a mass balance corresponding to aromaticity loss during
476 paracetamol ozonation is considered (Eq. 6). It is also assumed that reduction of water
477 aromaticity follows first-order kinetics.

478

$$479 \quad \frac{d[\text{Arom}]}{dt} = -k_A [\text{Arom}] \quad (6)$$

480

481 being,

482

483 [Arom]: water aromaticity (AU)

484 t: time (min)

485

486 By integrating the mass balance (Eq. 7), the kinetic equation corresponding to
487 aromaticity loss can be obtained (Eq. 8):

488

$$489 \quad \int_{\text{Arom}_0}^{\text{Arom}} \frac{d[\text{Arom}]}{[\text{Arom}]} = -k_A \int_{t=0}^t dt \quad (7)$$

490

$$491 \quad [\text{Arom}] = [\text{Arom}]_0 \exp(-k_A t) \quad (8)$$

492

493 In Fig. 6, both predicted and experimental results on aromaticity loss are shown, these
494 allowing the estimation of the first-order kinetic constant describing aromaticity loss
495 (k_A , 1/min) as a function of the pH (Eq. 9). On the other hand, it is verified that
496 aromaticity of ozonized samples at the end of the treatment does not depend on initial
497 pH, estimating a mean value for this parameter in the order of 0.06 AU (Eq. 10) that it

498 has been depreciated in the proposed model. Table 1 gathers the values of the estimated
499 kinetic parameters.

500

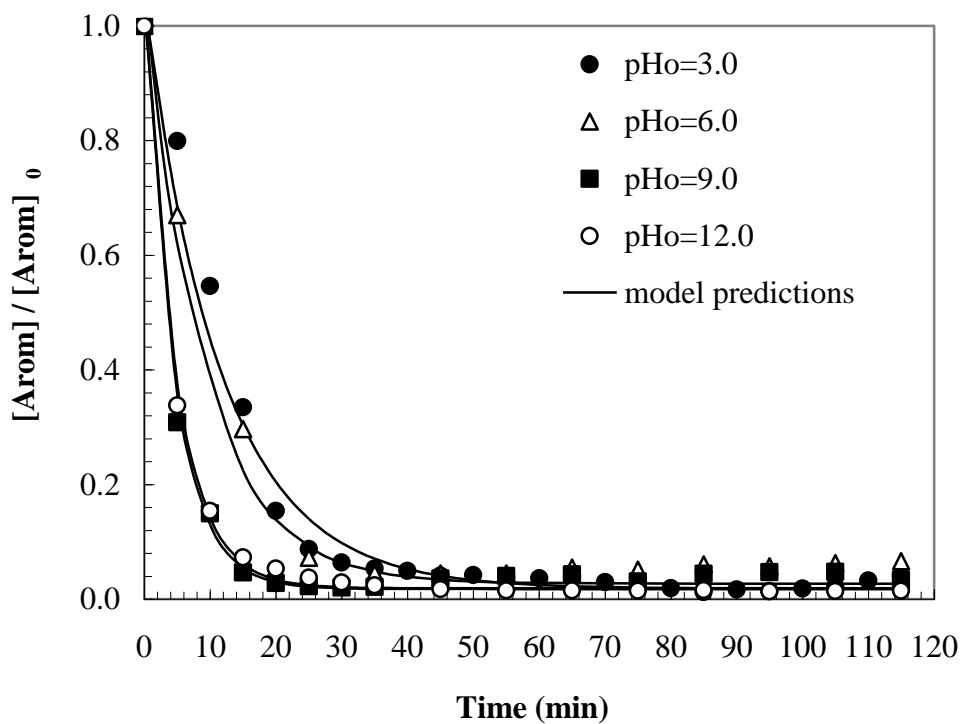
501 $k_A = 0.0162 \text{ pH} + 0.035$ (9)

502 $r^2=0.9301$

503

504 $[\overline{\text{Arom}}]_{\infty} = 0.06 \text{ (AU)}$ (10)

505



506

507 **Fig. 6.** Effect of initial pH on aromaticity loss for ozonized paracetamol solutions.
508 Experimental conditions: $P_{a0}=50.0 \text{ mg/L}$; $[O_3]=25.0 \text{ mg/min}$; $T=25.0^\circ\text{C}$.

509

510 Color changes taking place in water during paracetamol ozonation have been modelled
511 based on studies reported in the bibliography about the changes of color observed in
512 aqueous solutions of organic compounds oxidized by Fenton technologies (Villota et al.,
513 2018), following the scheme shown in Eq. 11. As mentioned, colorless aqueous

514 solutions of this pharmaceutical acquire a strong reddish tonality that turns to yellow
 515 when waters exhibit their maximum degree of coloration ($Color_{max}$). The rate of color
 516 formation has been expressed as a function of the kinetic constant k_f (1/min). Then,
 517 color is gradually degraded until a residual tonality is reached ($Color_{\infty}$). The velocity of
 518 color degradation is given by the corresponding first-order kinetic constant, k_d (1/min).

519



521 Being,

522

523 $Color_0$: initial color of paracetamol aqueous solutions (AU)

524 $Color_{max}$: maximum intensity presented by oxidized paracetamol solutions (AU)

525 $Color_{\infty}$: color of oxidized paracetamol solutions at the end of treatment (AU)

526 k_f : first-order kinetic constant for color formation during paracetamol
 527 ozonation (1/min).

528 k_d : first-order kinetic constant for color degradation during paracetamol
 529 ozonation (1/min).

530 t_0 : initial time (min)

531 t_{max} : time for which treated solutions show a maximum in color intensity (min).

532 t_{∞} : time corresponding to end of treatment (min)

533

534 According to the reaction scheme proposed in Eq. 11, the mass balances corresponding
 535 to color formation-degradation processes have been applied (see Eqs. 12-13).

536

537
$$\frac{d\text{Color}}{dt} = k_f (\text{Color} + \text{Color}_0) \int_{\text{Color}_0}^{\text{Color}_{\max}} \quad (12)$$

538

539
$$\frac{d\text{Color}}{dt} = -k_d (\text{Color} + \text{Color}_\infty) \int_{\text{Color}_{\max}}^{\text{Color}_\infty} \quad (13)$$

540 Considering the fact that color evolves according to first-order kinetics, mass balances
 541 above expressed have been both integrated to obtain explicit kinetic expressions for
 542 color formation (Eq. 14) and degradation (Eq. 15).

543

544
$$\text{Color} = 2 \text{Color}_0 \exp(k_f t) - \text{Color}_0 \int_{\text{Color}_0}^{\text{Color}_{\max}} \quad (14)$$

545

546
$$\text{Color} = (\text{Color}_{\max} - \text{Color}_\infty) \exp[-k_d (t - t_{\max})] + \text{Color}_\infty \int_{\text{Color}_{\max}}^{\text{Color}_\infty} \quad (15)$$

547

548 In Fig. 7, predictions made according to the proposed model are shown. Table 1 also
 549 gathers the values of the estimated kinetic parameters. Obtained results allow
 550 concluding that the kinetic constant describing color formation (k_f , 1/min) does not
 551 depend on pH. In fact, a mean value of $k_f=0.01$ 1/min could be estimated (Eq. 16).
 552 However, the kinetic constant for color degradation presents a linear dependency with
 553 operation pH (Eq. 17). This fact could be explained as follows: despite the treatment
 554 conditions appear to be powerful enough to degrade paracetamol molecules to colored
 555 transformation species, further degrading these intermediates to colorless byproducts
 556 could require a more severe oxidation. Because of this, in order to increase the rate of
 557 color degradation it is necessary to favor –during ozonation process– the generation of
 558 more oxidizing species (*i.e.*, hydroxyl radicals) by taking advantage of the pH effect.

559

560 $\bar{k}_f = 0.01 \text{ (1/min)}$ (16)

561

562 $k_d = 0.03 \text{ pH}_0 - 0.055$ (17)

563 $r^2=0.9783$

564

565 The influence of operational pH on the color of the treated water has been also assessed
566 (Eqs. 18-20). As can be seen, this color intensity gets larger with increasing operation
567 pH due to the fact that a higher concentration of oxidizing species is generated, causing
568 the degradation of paracetamol to chromophoric reaction intermediates. In a similar
569 way, the residual color at the end of the treatment is less intense when the reaction is
570 carried out under basic medium conditions. This is explained by an enhancement in the
571 oxidation efficiency of the process, leading to the generation of more hydroxyl radicals
572 per consumed ozone, which allows a further oxidation of colored species to colorless
573 degradation products. Therefore, the time for which the oxidized water reaches its peak
574 color intensity diminishes with increasing operational pH.

575

576 $\text{Color}_0 = 0.0006 \text{ pH}_0 + 0.006$ (18)

577 $r^2=0.9818$

578

579 $\text{Color}_{\text{max}} = 0.0016 \text{ pH}_0^2 - 0.0139 \text{ pH}_0 + 0.0378$ (19)

580 $r^2=0.9995$

581

582 $\text{Color}_\infty = 0.002 - 0.0004 \text{ pH}_0$ (20)

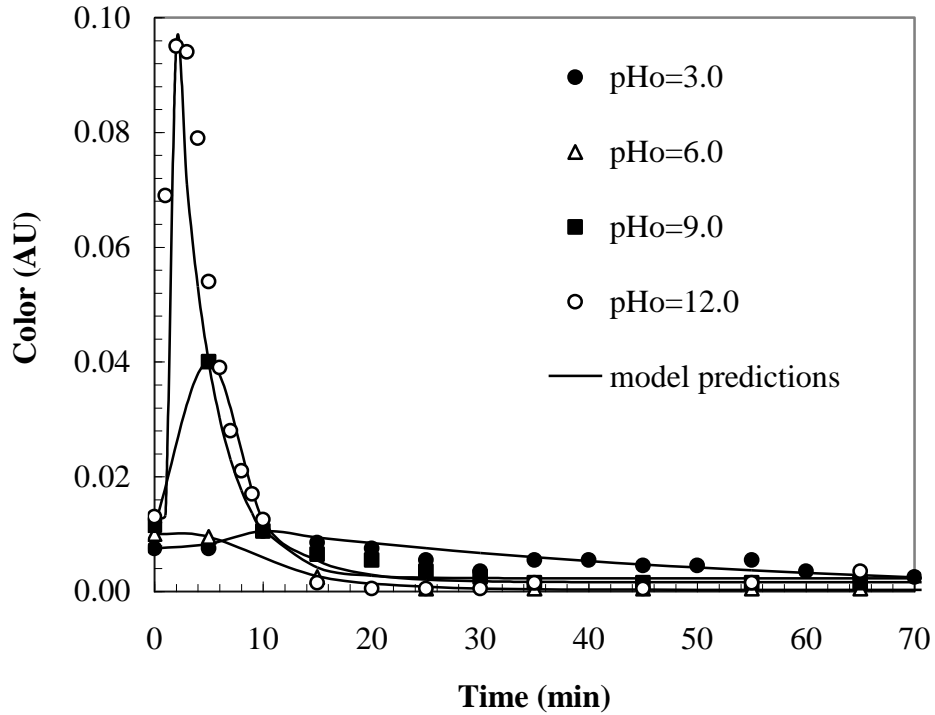
583 $r^2=0.9831$

584

585 $t_{\max} = 17.321 \exp(-0.1745 \text{pH}_0)$ (21)

586 $r^2=0.9884$

587



588

589 **Fig. 7.** Influence of initial pH on water color formation during ozonation of paracetamol
 590 aqueous solutions. Experimental conditions: $\text{Pa}_0=50.0 \text{ mg/L}$; $[\text{O}_3]=25.0 \text{ mg/min}$;
 591 $T=25.0^\circ\text{C}$.

592

593 According to the previous estimations, a parameter α (Eq. 23) expressing the
 594 relationship between formed color and aromaticity loss as a function of pH has been
 595 defined. To do so, the kinetic constants k_f (1/min) and k_A (1/min) have been both
 596 considered, as expressed in Eq. 22.

597

598 $k_A = \alpha k_f$ (22)

599

600 $\alpha = 1.62 \text{pH}_0 + 3.5$ (23)

601

602 **Table 1.** Estimated kinetic parameters. Experimental conditions: $[Pa]_0=50.0$ mg/L;
603 $[O_3]=25.0$ mg/min; $T=25.0^\circ C$.

604

pH₀	Color₀ (AU)	Color_{max} (AU)	Color_∞ (AU)	t_{max} (min)	k_f (1/min)	k_d (1/min)	[Arom]_∞ (AU)	k_A (1/min)
3.0	0.0075	0.0105	0.0000	10	0.01	0.02	0.050	0.085
6.0	0.0100	0.0095	0.0003	6	0.01	0.15	0.070	0.110
9.0	0.0115	0.0400	0.0016	4	0.01	0.21	0.050	0.220
12.0	0.0130	0.0950	0.0023	2	0.01	0.30	0.060	0.210

605

606 **4. Conclusions**

607 The ozonation of paracetamol aqueous solutions produces in a first stage a strong red
608 coloration at the same time that water aromaticity decreases. Then, a second stage takes
609 place; color intensity diminishes until it reaches a residual yellow tonality. This color
610 formation is favored when operating at $pH_0=12.0$ and ozone flow-rates applied in the
611 range 4.2 mg/min. The ozonation of aqueous solutions of paracetamol leads to
612 compounds such as p-aminophenol, p-nitrophenol, nitrocatechol, hydroquinone and
613 benzoquinone.

614

615 The hydroxide ions activate ozone decomposition to hydroxyl radicals, as well as to the
616 increasing degree of dissociation of paracetamol lead to the generation of chromophoric
617 structures. Ozone transfer to water is maximum when operating at $pH_0=6.0$, being this
618 explained by the presence, at higher pH values, of larger amounts of the hydroxide
619 anion and a possible generation of inorganic salts acting as scavengers for ozone and
620 hydroxyl radicals.

621

622 A first order kinetic for water color changes fits well the experimental results. The
623 obtained kinetic constants for color formation and degradation were to be $k_f=0.01$
624 (1/min) and $k_d=0.03 \text{ pH}_0-0.055$ (1/min), respectively. Finally, the aromaticity loss is
625 related to color changes. The corresponding first-order kinetic constant for aromaticity
626 is given by $k_A=0.0162 \text{ pH}_0+0.035$ (1/min).

627

628 **Acknowledgements**

629

630 This work was financially supported by the Spanish Ministry of Economy and
631 Competitiveness (project CTQ2014-52607-R), the Agency for Management of
632 University and Research Grants of the Government of Catalonia (project 2014SGR245),
633 and the Department of Chemical Engineering of the University of the Basque County
634 UPV/EHU.

635

636 **References**

637

638 Ay, F., Kargi, F., 2011. Effects of reagent concentrations on advanced oxidation of
639 amoxicillin by photo-Fenton treatment. *J. Environ. Eng-Asce.* 137(6):472-480.
640 [https://10.1061/\(ASCE\)EE.1943-7870.0000344](https://10.1061/(ASCE)EE.1943-7870.0000344).

641

642 Baalbaki, Z., Sultana, T., Maere T., Vanrolleghem, P., Metcalfe, C.D., Yargeau, V.,
643 2016. Fate and mass balance of contaminants of emerging concern during wastewater
644 treatment determined using the fractionated approach. *Sci. Total Environ.* 573:1147–
645 1158. <https://doi.org/10.1016/j.scitotenv.2016.08.073>.

646

647 Bader, H. Hoigné, J., 1981. Determination of ozone in water by the indigo method.
648 Water Res. 15:449-456. [https://doi.org/10.1016/0043-1354\(81\)90054-3](https://doi.org/10.1016/0043-1354(81)90054-3).
649
650 Bahnemann, W., Muneer, M., Haque, M.M., 2007. Titanium dioxide-mediated
651 photocatalyzed degradation of selected organic pollutants in aqueous suspensions,
652 Catal. Today 124:133–148. <https://doi.org/10.1016/j.cattod.2007.03.031>.
653
654 Blair, B., Nikolaus, A., Hedman, C., Klaper, R., Grundl, T., 2015. Evaluating the
655 degradation, sorption, and negative mass balances of pharmaceuticals and personal care
656 products during wastewater treatment. Chemosphere 134:395–401.
657 <https://doi.org/10.1016/j.chemosphere.2015.04.078>.
658
659 Brunet, R., Bourbigot, M.M., Dore, M., 1982. The Influence of the Ozonation Dosage
660 on the Structure and Biodegradability of Pollutants in water, and its Effect on Activated
661 Carbon Filtration. Ozone Sci. Eng. 4:15-32.
662 <https://doi.org/10.1080/01919518208550935>.
663
664 Can, Z.S., Gurol, M., 2003. Formaldehyde formation during ozonation of drinking
665 water. Ozone-Sci. Eng. 25:41-51. <https://doi.org/10.1080/713610649>.
666
667 Cruz-Alcalde, A., Sans, C., Esplugas, S., 2017. Priority pesticides abatement by
668 advanced water technologies: The case of acetamiprid removal by ozonation. Sci. Total
669 Environ. 599–600:1454–1461. <https://doi.org/10.1016/j.scitotenv.2017.05.065>.
670

671 Dastmalchi, S., Rashidi, M.R., Rassi, M., 1995. Simultaneous determination of the pK_a
672 and octanol/water partition coefficient of acetaminophen. J. School Pharm. Med. Sci.
673 Univ. Tehran. 4:7-14.
674

675 Deblonde, T., Hartemann, P., 2013. Environmental impact of medical prescriptions:
676 assessing the risks and hazards of persistence, bioaccumulation and toxicity of
677 pharmaceuticals. Public Health 127:312-317.
678 <https://doi.org/10.1016/j.puhe.2013.01.026>.
679

680 El Najjar, N.H., Touffet, A., Deborde, M., Journel, R., Karpel Vel Leitner, N., 2014.
681 Kinetics of paracetamol oxidation by ozone and hydroxyl radicals, formation of
682 transformation products and toxicity. Sep. and Purif. Technol. 136:137-143.
683 <https://doi.org/10.1016/j.seppur.2014.09.004>.
684

685 Ellenhorn, M.J., Barceloux, D.G. 1988. Medical Toxicology: Diagnosis and Treatment
686 of Human Poisoning. Elsevier Science, New York.
687

688 Gomes, J., Costa, R., Quinta-Ferreira, R.M., Martins, R.C. 2017. Application of
689 ozonation for pharmaceuticals and personal care products removal from water. Sci.
690 Total Environ. 586:265-283. <https://doi.org/10.1016/j.scitotenv.2017.01.216>.
691

692 Gottschalk, C., Libra, J.A., Saupe, A., 2010. Ozonation of Water and Waste Water. A
693 Practical Guide to Understanding Ozone and its Applications, second ed. Wiley- VCH,
694 Weinheim. <https://doi.org/10.1002/9783527628926>.
695

696 Greenberg, A.E., Eaton, A.D., Clesceri, L.S., 1999. Method 4500-O3 (ozone residual)
697 Indigo colorimetric method, in: Stand. Methods Exam. Water Wastewater, 20th Ed.,
698 American Public Health Association.
699

700 He, W.L., Wu, C.D., 2018. Incorporation of Fe-phthalocyanines into a porous organic
701 framework for highly efficient photocatalytic oxidation of arylalkanes. Appl. Catal. B-
702 Environ. 234:290-295. <https://doi.org/10.1016/j.apcatb.2018.04.055>.
703

704 Hollender, J., Zimmermann, S.G., Koepke, S., Krauss, M., Mcardell, C.S., Ort, C.,
705 Singer, H., Von Gunten, U., Siegrist, H., 2009. Elimination of organic micropollutants
706 in a municipal wastewater treatment plant upgraded with a full-scale post-ozonation
707 followed by sand filtration. Environ. Sci. Technol. 43:7862–7869.
708 <https://doi.org/10.1021/es9014629>.
709

710 Lee, Y., Gerrity, D., Lee, M., Gamage, S., Pisarenko, A., Trenholm, R.A., Cononica, S.,
711 Snyder, S.A., von Gunten, U., 2016. Organic contaminant abatement in reclaimed water
712 by UV/H₂O₂ and a combined process consisting of O₃/H₂O₂ followed by UV/H₂O₂:
713 Prediction of abatement efficiency, energy consumption and byproduct formation.
714 Environ. Sci. Technol. 50:3809–3819. <https://doi.org/10.1021/acs.est.5b04904>.
715

716 Lee, Y., von Gunten, U. 2016. Advances in predicting organic contaminant abatement
717 during ozonation of municipal wastewater effluent: Reaction kinetics, transformation
718 products, and changes of biological effects. Environ. Sci. Water Res. Technol. 2:421–
719 442. <https://doi.org/10.1039/C6EW00025H>.
720

721 Marcé, M., Domenjoud, B., Esplugas, S., Baig, S. 2016. Ozonation treatment of urban
722 and biotreated wastewaters: Impacts and modelling. *Chem. Eng. J.* 283:768-777.
723 <https://doi.org/10.1016/j.cej.2015.07.073>.
724

725 Margot, J., Kienle, C., Magnet, A., Weil, M., Rossi, L., de Alencastro, L.F., Abegglen,
726 C., Thonney, D., Chevre, N., Schearer, M., Barry, D.A., 2013. Treatment of
727 micropollutants in municipal wastewater: Ozone or powdered activated carbon? *Sci.*
728 *Total Environ.* 461–462:480–498. <https://doi.org/10.1016/j.scitotenv.2013.05.034>.
729

730 Martignac, M., Oliveros, E., Maurette, M.T., Claparols, C., Benoit-Marquie, F., 2013.
731 Mechanistic pathways of the photolysis of paracetamol in aqueous solution: an example
732 of photo-Fries rearrangement. *Photoch. Photobio. Sci.* 12(3):527-535.
733 <https://doi.org/10.1039/c2pp25341k>.
734

735 Maya, N., Evans, J., Nasuhoglu, D., Isazadeh, S., Yargeau, V., Metcalfe, C.D., 2018.
736 Evaluation of Wastewater Treatment by Ozonation for Reducing the Toxicity of
737 Contaminants of Emerging Concern to Rainbow Trout (*Oncorhynchus mykiss*).
738 *Environ. Toxicol. and Chem.* 37(1):274–284.

739 McEvoy, G.K., 1992. *American Hospital Formulary Service—Drug Information*, 92,
740 *Am. Soc. Hospital Pharmacists, Inc., Bethesda, MD.* <https://doi.org/10.1002/etc.3952>.
741

742 Mijangos, F., Varona, F., Villota, N., 2006. Changes in solution color during phenol
743 oxidation by Fenton reagent. *Environ. Sci. Technol.* 40:5538-5543.
744 <https://doi.org/10.1021/es060866q>.
745

746 Moctezuma, E, Leyva, E, Aguilar, C.A., Luna, R.A., Montalvo, C., 2012. Photocatalytic
747 degradation of paracetamol: Intermediates and total reaction mechanism. *J. Hazard.*
748 *Mater.* 243:130-138. <https://doi.org/10.1016/j.jhazmat.2012.10.010>.
749

750 Moctezuma, E., Leyva, E., Palestino, G., de Lasa, H., 2007. Photocatalytic degradation
751 of methyl parathion: reaction pathways and intermediate reaction products, *J.*
752 *Photochem. Photobiol. A: Chem.* 186:71–84.
753 <https://doi.org/10.1016/j.jphotochem.2006.07.014>.

754 Mompelat, S., Le Bot, B., Thomas, O., 2009. Occurrence and fate of pharmaceutical
755 products and by-products from resource to drinking water. *Environ. Int.*, 35:803-814.
756 <https://doi.org/10.1016/j.envint.2008.10.008>.
757

758 Nawrocki, J., Kasprzyk-Hordern, B., 2003. Comments on "Solid phase catalytic
759 ozonation process for the destruction of a model pollutant" by D.S. Pines and D.A
760 Reckhow - (*Ozone Sci. Eng.* 25 (2003); 25). *Ozone-Sci. Eng.* 25: 535-537.
761 <https://doi.org/10.1080/01919510390481847>.
762

763 Oller, I., Malato, S., Sánchez-Pérez, J.A., 2011. Combination of Advanced Oxidation
764 Processes and biological treatments for wastewater decontamination--a review. *Sci.*
765 *Total Environ.* 409(20):4141-66. <https://doi:10.1016/j.scitotenv.2010.08.061>.
766

767 Paraskeva, P., Graham, N.J.D., 2002. Ozonation of municipal wastewater effluents.
768 *Water Environ. Res.* 74:569-581. <https://doi.org/10.2175/106143002x140387>.
769

770 Radjenović, J., Petrović, M., Barceló, D., 2009. Complementary mass spectrometry and
771 bioassays for evaluating pharmaceutical-transformation products in treatment of
772 drinking water and wastewater. *Trac-Trend. Anal. Chem.*, 28:562-582.
773 <https://doi.org/10.1016/j.trac.2009.02.006>.
774

775 Rauert, C., Harner, T., Schuster, J.K., Eng, A., Fillmann, G., Castillo, L.E., Fentanes,
776 O., Villa Ibarra, M., Miglioranza, K.S.B., Moreno Rivadeneira, I-, Pozo, K., Aristizabal
777 Zuluaga, B.H., 2018. Atmospheric Concentrations of New Persistent Organic Pollutants
778 and Emerging Chemicals of Concern in the Group of Latin America and Caribbean
779 (GRULAC) Region. *Environ. Sci. Technol.*, 52(13):7240-7249.
780 <https://doi.org/10.1021/acs.est.8b00995>.
781

782 Reemtsma, T., These, A., 2005. Comparative investigation of low-molecular-weight
783 fulvic acids of different origin by SEC-Q-TOF-MS: New insights into structure and
784 formation. *Environ. Sci. Technol.* 39: 3507-3512. <https://doi.org/10.1021/es0480466>.
785

786 Richardson, S.D., 2009. Water analysis: emerging contaminants and current issues.
787 *Anal. Chem.*, 81:4645-4677. <https://doi.org/10.1021/acs.analchem.7b04577>.
788

789 Rodríguez, A., Rosal, R., Perdigón-Melón, J.A., Mezcua, M., Agüera, A., Hernando,
790 M.D., Letón, P., Fernández-Alba, A.R., García-Calvo, E., 2008. Ozone-Based
791 technologies in water and wastewater treatment. *Handbook Environ. Chem.* 5:127-175.
792 https://doi.org/10.1007/698_5_103.
793

794 Rodríguez, C., Lombraña, J.I., de Luis, A., Sanz, J., 2017. Oxidizing efficiency analysis
795 of an ozonation process to degrade the dye rhodamine 6G. *J. Chem. Technol.*
796 *Biotechnol.* 92:674–683. <https://doi.org/doi:10.1002/jctb.5051>.

797 Rosario-Ortiz, F.L., Wert, E.C., Snyder, S.A., 2010. Evaluation of UV/H₂O₂ treatment
798 for the oxidation of pharmaceuticals in wastewater. *Water Res.* 44:1440–1448.
799 <https://doi.org/10.1016/j.watres.2009.10.031>.

800 Roth J.A. and Sullivan D.E., 1981. Solubility of ozone in water. *Ind Eng Chem Fundam*
801 20:137–140. <https://doi.org/10.1021/i100002a004>.

802

803 Santos, L., Araùjo, A.N., Fachini, A., Pena, A., 2010. Ecotoxicological aspects related
804 to the presence of pharmaceuticals in the aquatic environment. *J. Hazard. Mater.*
805 175:45-95. <https://doi.org/10.1016/j.jhazmat.2009.10.100>.

806

807 Savchuk, N., Krizova, P., 2015. Membrane and AOP processes-their application and
808 comparison in treatment of wastewater with high organics content. *Desalin. Water*
809 *Treat.* 56:3247-3251. <https://doi.org/10.1080/19443994.2014.980978>.

810

811 Seifrtová, M., Nováková, L., Lino, C., Pena, A., Solich, P., 2009. An overview of
812 analytical methodologies for the determination of antibiotics in environmental waters.
813 *Anal. Chim. Acta* 649:158-179. <https://doi.org/10.1016/j.aca.2009.07.031>.

814

815 Skoumal, M., Cabot, P-L., Centellas, F., Arias, C., R.M., Garrido, J.A., Brillas, E.,
816 2006. Mineralization of paracetamol by ozonation catalyzed with Fe²⁺, Cu²⁺ and UVA
817 light. *App. Catal., B* 20:228-240. <https://doi.org/10.1016/j.apcatb.2006.03.016>.

818

819 Sumegova, L., Derco, J., Melicher, M., 2013. Influence of reaction conditions on the
820 ozonation process. *Acta Chim. Slovaca* 6:168-172. [https://doi.org/10.2478/acs-2013-](https://doi.org/10.2478/acs-2013-0026)
821 0026.
822

823 Sun, Q., Lv, M., Hu, A., Yang, X., Yu, C.P., 2014. Seasonal variation in the occurrence
824 and removal of pharmaceuticals and personal care products in a wastewater treatment
825 plant in Xiamen, China. *J. Hazard. Mater.* 277:69-75.
826 <https://doi.org/10.1016/j.jhazmat.2013.11.056>.
827

828 Swietlik, J., Sikorska, E., 2004. Application of fluorescence spectroscopy in the studies
829 of natural organic matter fractions reactivity with chlorine dioxide and ozone. *Water*
830 *Res.* 38: 3791-3799. <https://doi.org/10.1016/j.watres.2004.06.010>.
831

832 Valdés, M.E., Amé, M.V., Bistoni, M.M, Wunderlin, D.A., 2014. Occurrence and
833 bioaccumulation of pharmaceuticals in a fish species inhabiting the Suquía River basin
834 (Córdoba, Argentina). *Sci. Total Environ.* 472:389-396.
835 <https://doi.org/10.1016/j.scitotenv.2013.10.124>.
836

837 Villaroel, E., Silva-Agreto, J., Petrier, C., Taborda, G., Torres-Palma, R., 2014.
838 Ultrasonic degradation of acetaminophen in water: Effect of sonochemical parameters
839 and water matrix. *Ultrason. Sonochem.* 21:1763-1769.
840 <http://dx.doi.org/10.1016/j.ultsonch.2014.04.002>.
841

842 Villota, N., Lomas, J.M., Camarero, L.M., 2016. Study of the paracetamol degradation
843 pathway that generates color and turbidity in oxidized wastewaters by photo-Fenton

844 technology. J. Photochem Photobiol A Chem. 329:113–119.
845 <https://doi.org/10.1016/j.jphotochem.2016.06.024>.
846
847 Villota, N., Lomas, J.M., Camarero, L.M., 2018. Kinetic modelling of water-color
848 changes in a photo-Fenton system applied to oxidate paracetamol. J. Photochem
849 Photobiol A Chem. 356:573–579. <https://doi.org/10.1016/j.jphotochem.2018.01.040>.
850
851 Vogna, D., Marotta, R., Napolitano, A., d'Ischia, M., 2002. Advanced oxidation
852 chemistry of paracetamol. UV/H₂O₂-induced hydroxylation/degradation pathways and
853 ¹⁵N-aided inventory of nitrogenous breakdown products, J. Org. Chem. 67:6143–6151.
854 <https://doi.org/10.1021/jo025604v>.
855
856 von Gunten, U., 2003. Ozonation of drinking water: Part I. Oxidation kinetics and
857 product formation. Water Res. 37:1443–1467. [https://doi.org/10.1016/S0043-](https://doi.org/10.1016/S0043-1354(02)00457-8)
858 [1354\(02\)00457-8](https://doi.org/10.1016/S0043-1354(02)00457-8).
859 Wert, E.C., Rosario-Ortiz, F.L., Drury, D.D., Snyder, S.A., 2007. Formation of
860 oxidation byproducts from ozonation of wastewater. Water Res. 41:1481–1490.
861 <https://doi.org/10.1016/j.watres.2007.01.020>.
862
863 Westerhoff P., Debroux J., Aiken G., Amy G., 1999. Ozone induced changes in natural
864 organic matter (nom) structure. Ozone Sci. Eng. 21: 551-570.
865 <https://doi.org/10.1080/01919512.1999.10382893>.
866 Xiong F., Legube B., 1991. Enhancement of radical chain reactions of ozone in waters
867 in the presence of an aquatic fulvic acid. Ozone Sci. Eng. 13:349-363.
868 <https://doi.org/10.1080/01919519108552471>.

869

870 Zenker, A., Cicero, M.R., Prestinaci, F., Bottoni, P., Carere, M., 2014. Bioaccumulation
871 and biomagnification potential of pharmaceuticals with a focus to the aquatic
872 environment. *J. Environ. Manage.* 133:378-387.
873 <https://doi.org/10.1016/j.jenvman.2013.12.017>.

874

875 Ziylan-Yavaş, A., Ince, N.H., 2018. Catalytic ozonation of paracetamol using
876 commercial and Pt-supported nanocomposites of Al₂O₃: The impact of ultrasound.
877 *Ultrason. Sonochem.* 40(B):175-182. <https://doi.org/10.1016/j.ultsonch.2017.02.017>.